journal

J. Am. Ceram. Soc., 96 [8] 2570–2576 (2013)
DOI: 10.1111/jace.12372

Effect of MgO and Y_2O_3 Doping on the Formation of Core–Shell Structure in $BaTiO_3$ Ceramics

Che-Yuan Chang, Wan-Ning Wang, and Chi-Yuen Huang†

Department of Resources Engineering, National Cheng Kung University, One University Road, Tainan City 70101, Taiwan

This study investigates the effects of doping $BaTiO_3$ with MgO and Y_2O_3 on the formation of core–shell structure. The MgO and Y_2O_3 enhanced the shrinkage upon sintering and inhibited the grain growth, respectively. However, increasing the amount of Y_2O_3 to 3.0 mol% suppressed the shrinkage upon sintering. The results of the diffusion experiment revealed that Y^{3+} was dissolved in the $BaTiO_3$ lattice to a depth of 5–10 nm inside the grains, whereas Mg^{2+} tended to remain close to the surfaces of the grains when sintered at 1150°C for 18 h, suggesting that Y^{3+} may have had a higher diffusion rate than Mg^{2+}. The Mg^{2+} prevented the diffusion of Y^{3+} into the core during sintering. Therefore, Mg^{2+} plays an important role as a shell maker in the formation of the core–shell structure in the codoped system. The core–shell structure can be obtained in $BaTiO_3$ ceramics that are codoped with MgO and Y_2O_3 upon sintering at 1150°C for 3 h.

I. Introduction

Barium titanate ($BaTiO_3$) is a ferroelectric perovskite ceramic that has a high permittivity at room temperature, making it suitable for applications in multilayer ceramic capacitors (MLCCs). However, the permittivity of pure $BaTiO_3$ ceramics varies dramatically with temperature, particularly approaching the phase transition temperature (−90°C, 0°C, and 125°C) and especially at the Curie temperature (T_c~125°C). Unstable changes in permittivity at the phase transition temperature can cause damage to electric devices. Previous studies have revealed two major ways to reduce these dramatic changes in permittivity. The first one involves modifying the phase transition temperature of $BaTiO_3$, and the other one involves flattening the capacitance curve. The phase transition temperature of $BaTiO_3$ is directly related to the composition. The flattening of the TCC curve is related to both compositional changes and the microstructure.[1–5]

Many studies have noted that using yttrium oxide (Y_2O_3) and magnesium oxide (MgO) as dopants can successfully modify the phase transition temperature and flatten the TCC curve of $BaTiO_3$ ceramics.[6–8] The ionic radius of Y^{3+} (1.0 Å) is between the radius of the Ba-site (1.61 Å) and that of the Ti-site (0.64 Å). In $BaTiO_3$, Y^{3+} can therefore substitute at both Ba-sites and Ti-sites. In a system with low concentrations (~0.5 mol%) of multidopants, the cell volume and T_c both have been found to increase with the amount of Y^{3+} that is substituted at the Ba-sites. The solubility limit of Y^{3+} at Ba-sites is approximately 2.0 mol%. As the concentration increases (>5 mol%), the crystalline phase of $BaTiO_3$ is transformed from tetragonal to pseudocubic. The tetragonality and T_c both decline when Y^{3+} is substituted at the Ti-sites. The solubility limit of Y^{3+} at the Ti-sites is about 12 mol%. A low dissipation factor is important in increasing the lifetime of $BaTiO_3$. Earlier studies have indicated that the incorporation of Y^{3+} into $BaTiO_3$ not only modifies the T_c but also reduces the dissipation factor (tan δ) of $BaTiO_3$ ceramics.[9–11] As mentioned above, the TCC curve can be flattened by changes in both composition and microstructure. The core–shell structure is a typical microstructure that flattens the TCC curve, in which the additive elements are partially dissolved in the BT lattice to form a shell that surrounds the core region. The shell is known to have a nonferroelectric pseudocubic structure, whereas the core is pure $BaTiO_3$ with a ferroelectric tetragonal structure. Magnesium oxide is widely used as a dopant in $BaTiO_3$ ceramics. The ionic radius of Mg^{2+} (0.72 Å) enables it to be substituted at the Ti-sites (0.64 Å) in $BaTiO_3$. A previous study revealed that rare-earth elements dissolved easily in $BaTiO_3$ whereas Mg tended to remain at grain boundary rather than being incorporated into $BaTiO_3$. Therefore, Mg^{2+} may play an important role as a shell maker in the formation of the core–shell structure. In addition, MgO and rare-earth oxides are known to improve the stability of the temperature dependence of the capacitance and also to have an important role in inhibiting the grain growth of $BaTiO_3$. Based on the experimental results, MgO was first precalcined with $BaTiO_3$ powder to form a shell structure before it was mixed with Y_2O_3.[12–14]

Many investigations have discussed the effect of the incorporation of MgO and Y_2O_3 on the dielectric properties of $BaTiO_3$. However, relatively few studies have addressed their effect on the microstructure of $BaTiO_3$. The main purpose of this study was to determine the effect of MgO and Y_2O_3 on the microstructure, respectively.

II. Experimental Procedure

The experiments were divided into two parts. The first part was the preparation of $BaTiO_3$ ceramics that were doped with MgO and Y_2O_3, respectively. Commercial $BaTiO_3$ powder (0.25 μm, Ba/Ti = 0.9967) was mixed with 0.5 or 1.0 mol% MgO (99%, Nanostructured & Amorphous Materials Inc., Houston, TX) using ball-milling, before being dried. The dried powder was pressed into disks with a diameter of 8 mm and a thickness of 3 mm. It was sintered at 1250°C for 3 h. The commercial $BaTiO_3$ powder was also mixed with 1.0 and 3.0 mol% Y_2O_3 (99.99%; Acros, Taipei, Taiwan) by ball-milling and then dried. The dried powder was pressed into disks and then sintered at 1250°C for 3 h. The second part of the experiment was the preparation of the $BaTiO_3$ ceramics that were codoped with MgO and Y_2O_3. Four samples were doped with various amounts of MgO and Y_2O_3, as shown in Table I. The commercial $BaTiO_3$ powder was first mixed with MgO by ball-milling and then dried. The dried powder was pre calcined at 800°C for 3 h and then mixed with Y_2O_3 by ball-milling. It was then pressed into disks and sintered at 1150°C–1250°C for 3 h. The diffusion experiments were performed using sintered

N. Alford—contributing editor

Manuscript No. 32348. Received November 28, 2012; approved April 8, 2013.
†Author to whom correspondence should be addressed. e-mail: cyhuang@mail.ncku.edu.tw

Table I. Composition of Four Samples Doped with Different Amounts of MgO and Y_2O_3 (mol%)

Notation	$BaTiO_3$	MgO	Y_2O_3
0.5Mg	99.5	0.5	0
1Mg	99.0	1.0	0
1Y	99.0	0	1.0
3Y	97.0	0	3.0
0.5Mg1Y	98.5	0.5	1.0
0.5Mg3Y	96.5	0.5	3.0
1Mg1Y	98.0	1.0	1.0
1Mg3Y	96.0	1.0	3.0

(1250°C/3 h) bulk $BaTiO_3$ and MgO or Y_2O_3 powder. The polished bulk sintered $BaTiO_3$ was placed on the MgO or Y_2O_3 powder and then heated to 1150°C with various dwelling times. A focus ion beam (FIB) was used to prepare the cross-section samples, and TEM was used to observe the depths of diffusion of Mg^{2+} and Y^{3+}.

The rates of shrinkage of the samples upon sintering were determined using a dilatometer (Dilatometer, 402C, Netzsch, Taipei, Taiwan). After sintering, the apparent densities of the samples were measured using Archimedes method. The microstructures were observed by high-resolution scanning electronic microscopy (HR-SEM, SU8000, Hitachi, Tokyo, Japan) and transmission electron microscopy (TEM; G^2-F20, FEI Philips, Tokyo, Japan). The average grain size was measured from SEM micrographs using Lucia measurement software (Laboratory Imaging, version 4.71). Each sample contained at least 200 grains.

III. Results and Discussion

Figure 1 plots the sintering shrinkage curves of $BaTiO_3$ that was doped with various amounts of MgO. The shrinkage curve of $BaTiO_3$ that was doped with 0.5 mol% MgO does not obviously differ from that of $BaTiO_3$. However, as the MgO concentration increases, the shrinkage curve of the sample that was doped with 1.0 mol% MgO shifts to a lower temperature, suggesting that MgO may enhance shrinkage upon sintering. Figure 2 plots the sintering shrinkage curves of $BaTiO_3$ that was doped with various amounts of Y_2O_3. The shrinkage curve of the sample that was doped with 1.0 mol% Y_2O_3 shifts to slightly lower temperature than that of $BaTiO_3$, but the curve that is obtained by doping with 3.0 mol% Y_2O_3 is shifted to a slightly higher temperature. Based on the sintering shrinkage curves in Fig. 2, adding

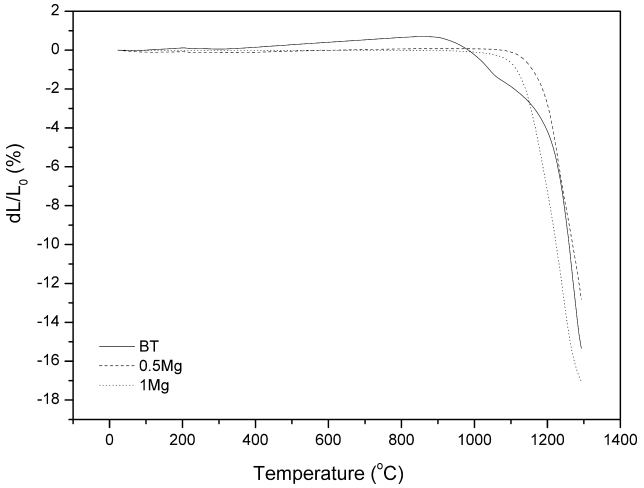

Fig. 1. Sintering shrinkage curves of $BaTiO_3$ doped with various amounts of MgO.

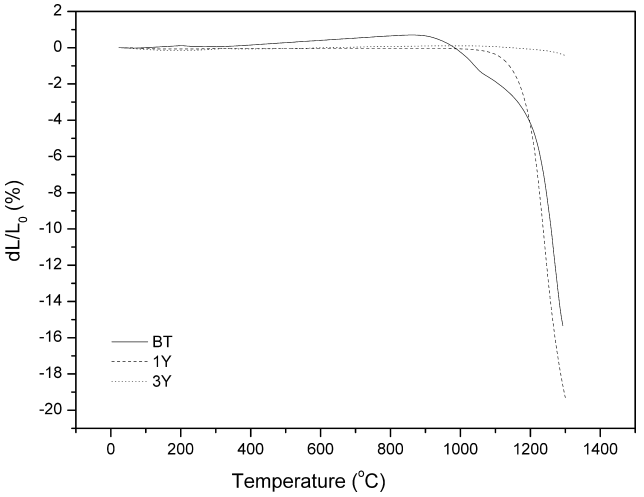

Fig. 2. Sintering shrinkage curves of $BaTiO_3$ dope with various amounts of Y_2O_3.

1.0 mol% Y_2O_3 can promote the shrinkage of $BaTiO_3$ ceramics upon sintering. However, the shrinkage upon sintering was suppressed when the amount of Y_2O_3 was increased to 3.0 mol%.

Based on the sintering shrinkage curves that are plotted in Figs. 1 and 2, 1250°C was chosen as the sintering temperature. Table II presents the relative density and average grain size. The sample that was doped with 1.0 mol% MgO has a higher relative density than the sample that was doped with 0.5 mol%. The sintering shrinkage curves in Fig. 1 indicate that the addition of 1.0 mol% MgO can improve the shrinkage upon sintering, yielding a higher relative density. The enhancement in the sintering shrinkage is attributable to the formation of oxygen vacancies. The oxygen vacancies are formed according to the following Eq. (1).

$$BaO + MgO \rightarrow Ba_{Ba} + Mg''_{Ti} + 2O_O + V_O^{\bullet\bullet} \quad (1)$$

Oxygen vacancies can increase the rate of diffusion during sintering. The rate of densification increases with the diffusion rate. Therefore, the samples that were doped with MgO have a higher relative density at a lower sintering temperature. Figures 3(a) and (b) show the SEM micrographs of $BaTiO_3$ that was doped with MgO that was sintered at 1250°C for 3 h. The samples that were doped with MgO both have smaller grains than $BaTiO_3$ following sintering at 1250°C for 3 h. As mentioned above, some of the Mg^{2+} dissolves into $BaTiO_3$, forming a solid solution, whereas the rest of Mg^{2+} reacts with $BaTiO_3$, forming a second phase of $MgTi_2O_5$ (Fig. 4). The formation of the second phase, $MgTi_2O_5$, at the grain boundaries may be responsible for the inhibition of the grain growth. This finding is similar to that supported by experimental results concerning $BaTiO_3$ that is doped with La_2O_3 that have been obtained in previous studies.[15,16] Therefore, the addition of MgO not only improves the shrinkage upon sintering but also inhibits the grain growth of $BaTiO_3$ during the final stage of sintering.

The sample that was doped with 1.0 mol% Y_2O_3 had a higher relative density than that doped with 3.0 mol% Y_2O_3, as shown in Table II. As the concentration of Y_2O_3 increases, the relative density decreases. The suppression of shrinkage upon sintering may be attributed to the formation of the second phase of $Y_2Ti_2O_7$ at the grain boundaries as shown in Fig. 5. The second phase may inhibit the grain growth during sintering. Lin *et al.* obtained the same results.[17] Hence, the sample that was doped with 3.0 mol% Y_2O_3 required a higher sintering temperature or a longer dwelling time. Figures 3(c) and (d) show the microstructures

Table II. Average Grain Size and Relative Density of $BaTiO_3$ Doped with MgO and Y_2O_3 Sintered at 1250°C for 3 h

	$BaTiO_3$ + 0.5MgO	$BaTiO_3$ + 1.0MgO	$BaTiO_3$ + 1.0Y_2O_3	$BaTiO_3$ + 3.0Y_2O_3	$BaTiO_3$
1250°C/3 h	0.35 μm (95%)	0.30 μm (98%)	0.75 μm (97%)	0.25 μm (60%)	1.0 μm (97%)

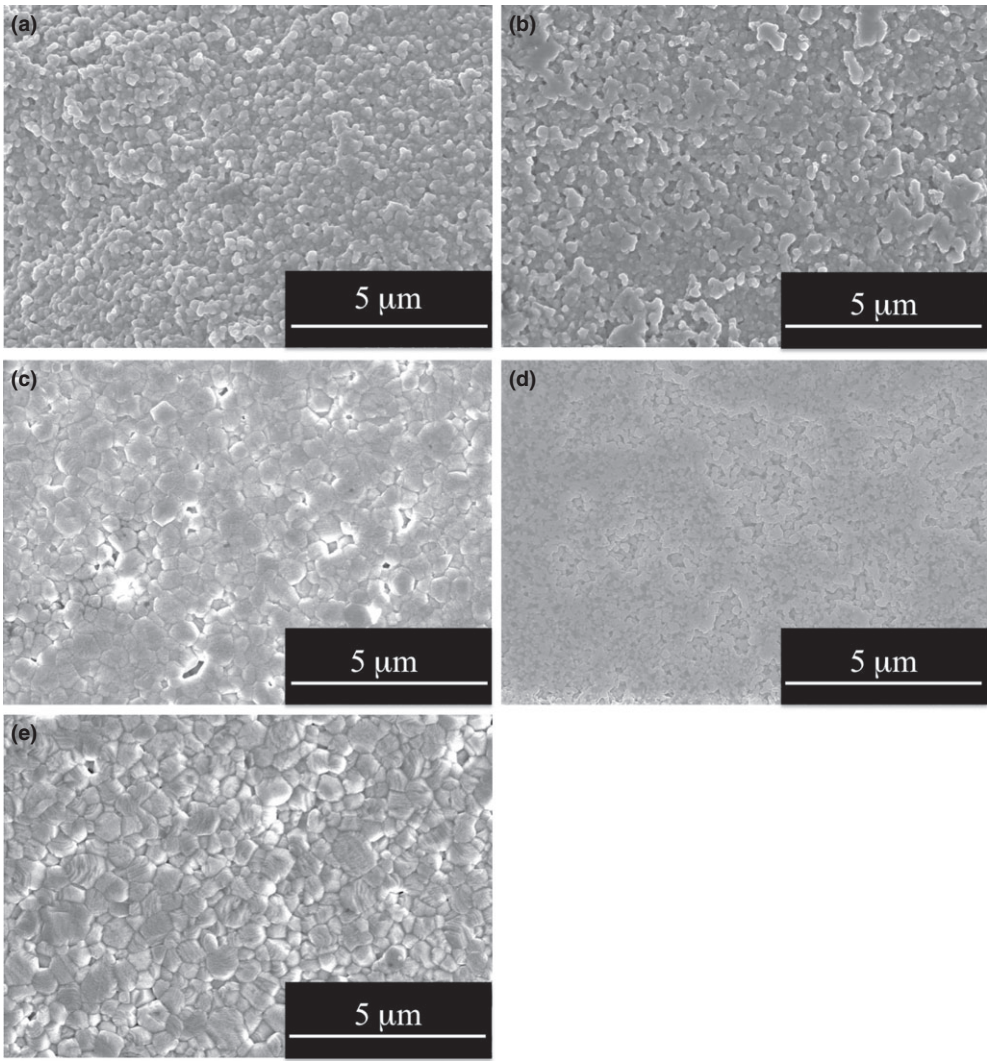

Fig. 3. SEM micrographs of $BaTiO_3$ doped with MgO and Y_2O_3 sintered at 1250°C for 3 h, respectively (a) $BaTiO_3$ + 0.5 mol% MgO (b) $BaTiO_3$ + 1.0 mol% MgO (c) $BaTiO_3$ + 1.0 mol% Y_2O_3 (d) $BaTiO_3$ + 3.0 mol% Y_2O_3 (e) $BaTiO_3$.

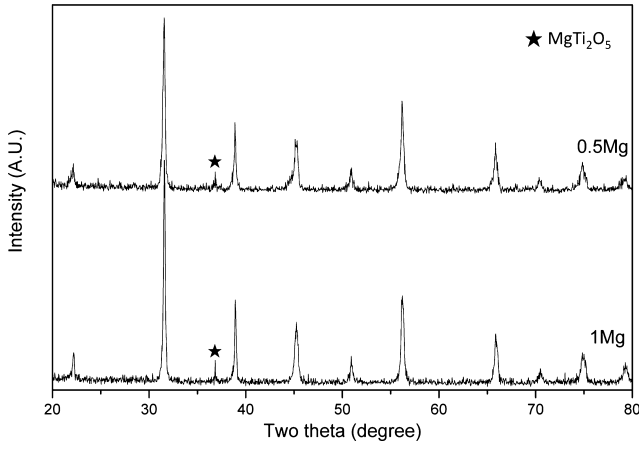

Fig. 4. The XRD patterns of $BaTiO_3$ doped with 0.5 and 1.0 mol% MgO sintered at 1250°C for 4 h.

of $BaTiO_3$ that was doped with various amounts of Y_2O_3 and sintered at 1250°C for 3 h. The sample that was doped with 1.0 mol% exhibited no obvious reduction in grain size. However, the grain size is dramatically reduced when 3.0 mol% Y_2O_3 is added. The SEM observations support the sintering shrinkage curve as shown in Fig. 2. The addition of 1.0 mol% Y_2O_3 can promote shrinkage upon sintering and suppress the grain growth of $BaTiO_3$ ceramics. However, increasing the amount of Y_2O_3 to 3.0 mol% suppressed the shrinkage.

The diffusion depths of Mg^{2+} and Y^{3+} depended on their diffusion rates. As Mg^{2+} and Y^{3+} diffused into $BaTiO_3$, the lattices became distorted, and the cell volumes increased, owing to their ionic radii. As observed in the HRTEM micrographs, the discontinuance of the lattice points indicated the positions of distortion or expansion of the cells. Figure 6 shows the HRTEM micrographs that were obtained in the diffusion experiments. The dashed lines in Fig. 6 represent the discontinuance of lattice points in all of the samples. Figures 6(a)–(c) show the bulks $BaTiO_3$ in contact with the

MgO powder that were sintered at 1150°C for various dwelling times. Small diffusion depths (1~2 nm) of Mg^{2+} in $BaTiO_3$ are observed. Even after a long dwelling time (18 h), the diffusion depth does not increase. The results demonstrate that the Mg^{2+} diffused slowly in the $BaTiO_3$ at temperatures under 1150°C. Figures 6(d)–(f) show the bulk $BaTiO_3$ in contact with the Y_2O_3 powder, heated to 1150°C for various dwelling times. The HRTEM images reveal that the diffusion depths increased with the dwelling time. In $BaTiO_3$, Y^{3+} clearly had a greater diffusion depth than Mg^{2+}. The results of the diffusion experiments verified that Mg^{2+} may have a lower diffusion rate than Y^{3+}, indicating that Mg^{2+} has a greater diffusion activation energy than Y^{3+} at temperatures under 1150°C. Therefore, Mg^{2+} has an important role as a shell maker in the core–shell structure at 1150°C. The formation of the shell structure on the $BaTiO_3$ surface reduced the diffusion rate of the other elements outside the shell, so the grain growth was inhibited.

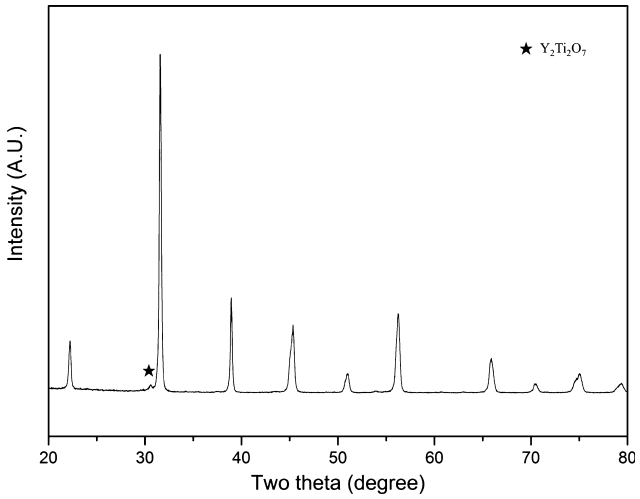

Fig. 5. The XRD pattern of $BaTiO_3$ doped with 3.0 mol% Y_2O_3 sintered at 1250°C for 3 h.

Figure 7 plots the sintering shrinkage curves of $BaTiO_3$ that was codoped with MgO and Y_2O_3. A comparison of Figs. 1 and 2 shows that the shrinkage temperatures of the three MgO–Y_2O_3-codoped samples, around 1150°C, were lower than that of 1Mg3Y. Figure 8 shows the SEM micrographs of $BaTiO_3$ codoped with MgO and Y_2O_3 sintered at 1150°C for 3 h. Table III presents the average grain sizes and relative densities obtained at various sintering temperatures. The average particle size of $BaTiO_3$ powder is about 0.25 μm, and no obvious grain growth occurred in the codoped samples. The grain sizes in $BaTiO_3$ that was doped with MgO were smaller than those in $BaTiO_3$. The inhibition of grain growth was associated with the formation of a shell structure that comprised MgO and $BaTiO_3$ on the $BaTiO_3$ surface. As mentioned above, the shell structure might have reduced the rate of diffusion of other elements outside the shell. Therefore, grain growth was inhibited when the shell structure was formed.

Figure 9 shows the TEM micrographs of $BaTiO_3$ that was codoped with MgO and Y_2O_3 and sintered at 1150°C for 3 h. The core–shell structure is observed in the dense ceramics 0.5Mg1Y, 0.5Mg3Y, and 1Mg1Y. Figure 9 also shows the TEM-EDS results of $BaTiO_3$ that was codoped with MgO and Y_2O_3 and sintered at 1150°C for 3 h. They reveal that the concentrations of Mg^{2+} and Y^{3+} in the shell exceed those in the core. Mg^{2+}, with a low diffusion rate, can suppress the diffusion of Y^{3+}. Based on the precalcination process, the shell structure that was formed from the $BaTiO_3$ that was doped with Mg^{2+} terminated the diffusion of Y^{3+}. The core–shell structure was successfully formed by the precalcination process. Figure 10 shows SEM micrographs of $BaTiO_3$ that was codoped with MgO and Y_2O_3 and sintered at 1250°C for 3 h. A comparison with Fig. 8 indicates that grain growth occurred in all samples when the sintering temperature was increased to 1250°C. As

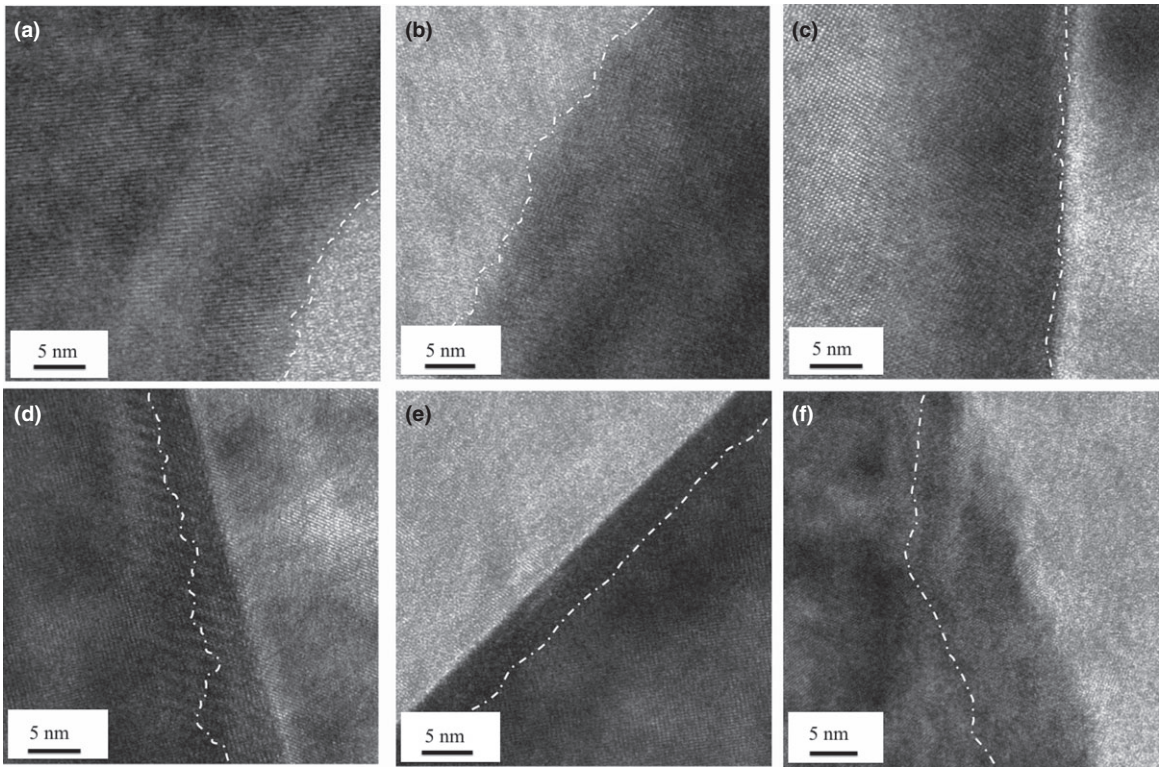

Fig. 6. The HRTEM micrographs of diffusion experiments heated to 1150°C with various dwelling times (a) $BaTiO_3$–MgO, 6 h, (b) $BaTiO_3$–MgO, 12 h, (c) $BaTiO_3$–MgO, 18 h, (d) $BaTiO_3$–Y_2O_3, 6 h, (e) $BaTiO_3$–Y_2O_3, 12 h (f) $BaTiO_3$–Y_2O_3, 18 h.

the sintering temperature was increased, more energy was provided to overcome the activation energy of diffusion. In addition, liquid phases formed in the samples 0.5Mg1Y and 1Mg1Y. Therefore, as sintering increased, Mg^{2+} may not stay in the shell region, but moved into the core region of the $BaTiO_3$, causing the core–shell structure to disappear. If no any other shell structure is present to block the elements outside the $BaTiO_3$, then the Mg^{2+} and Y^{3+} ions will homogeneously diffuse into the $BaTiO_3$ and initiate grain growth.

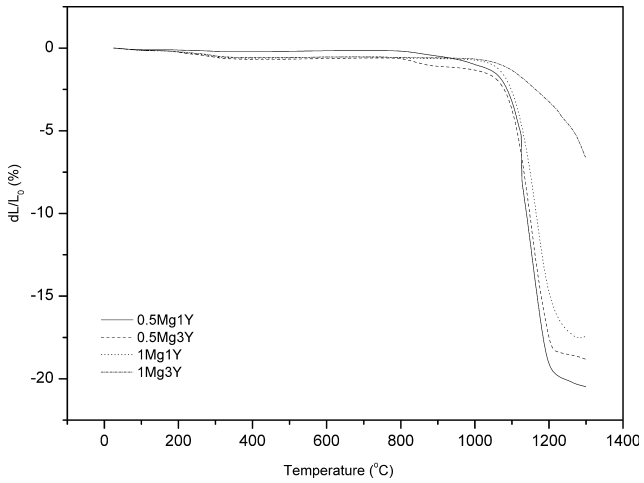

Fig. 7. Sintering shrinkage curves of $BaTiO_3$ codoped with MgO and Y_2O_3.

IV. Conclusions

The experimental results in the first part of this study verified the effects of doping with MgO and Y_2O_3 on the microstructure of $BaTiO_3$. Doping with MgO enhanced the shrinkage upon sintering by forming oxygen vacancies. When MgO was doped into $BaTiO_3$, the grain growth was inhibited by the formation of the second phase of $MgTi_2O_5$. Adding 1.0 mol% Y_2O_3 promoted the shrinkage upon sintering and suppressed the grain growth of $BaTiO_3$ ceramics. However, when the amount of Y_2O_3 was increased to 3.0 mol%, the formation of the second phase, $Y_2Ti_2O_7$, suppressed the shrinkage upon sintering. The diffusion experiments verified that the diffusion of Mg^{2+} in $BaTiO_3$ is more difficult than that of Y^{3+}. Mg^{2+} plays an important role as a shell maker.

The experimental results in the second part of this study verified the formation of a core–shell structure in $BaTiO_3$ ceramics that were codoped with MgO and Y_2O_3. The precalcination is an effective means of forming a core–shell structure, which can be obtained in dense ceramics 0.5Mg1Y, 0.5Mg3Y, and 1Mg1Y by sintering at 1150°C for 3 h.

Acknowledgment

The authors would like to thank the National Science Council of the Republic of China, Taiwan, for financially supporting this research under Contract No. NSC NSC100-2221-E-006-134-MY3.

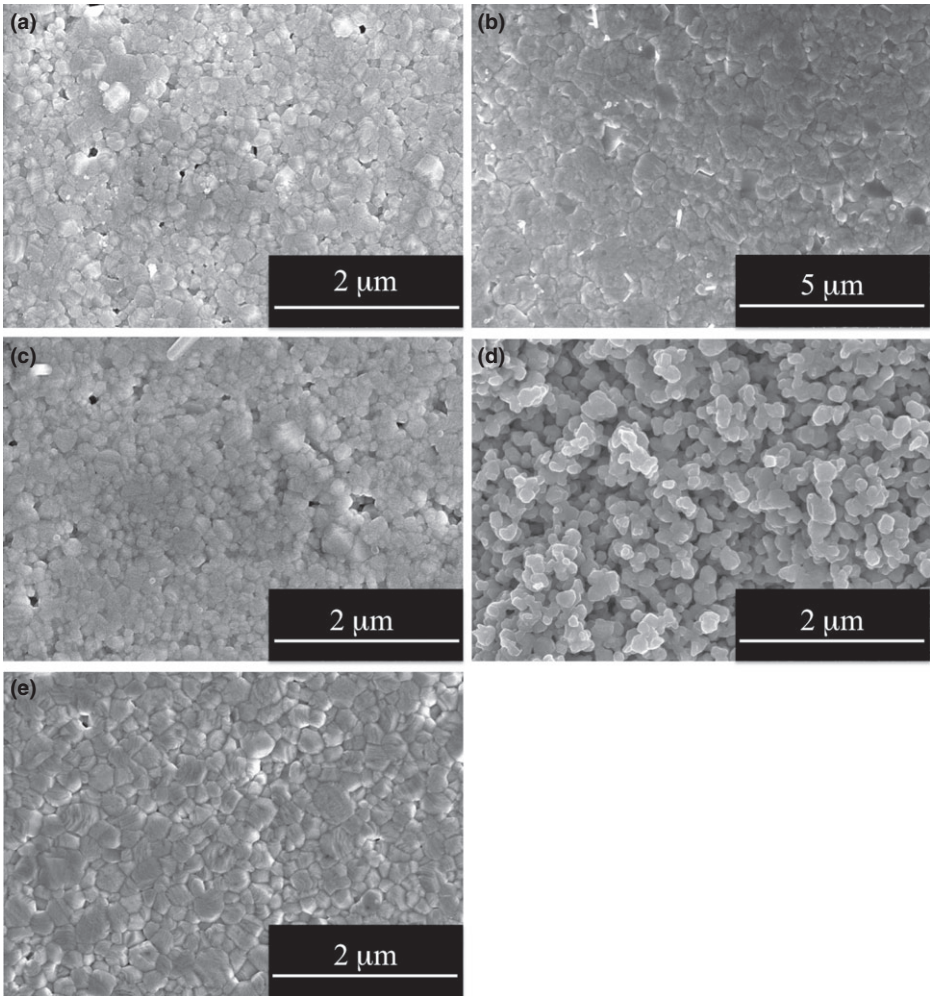

Fig. 8. SEM micrographs of $BaTiO_3$ codoped with MgO and Y_2O_3 sintered at 1150°C for 3 h, (a) 0.5Mg1Y, (b) 0.5Mg3Y, (c) 1Mg1Y, (d) 1Mg3Y, and (e) $BaTiO_3$.

Table III. Average Grain Size and Relative Density of $BaTiO_3$ Codoped with MgO and Y_2O_3 Sintered at 1150°C for 3 h

	0.5Mg1Y	0.5Mg3Y	1Mg1Y	1Mg3Y	$BaTiO_3$
1150°C/3 h	0.30 μm (92%)	0.45 μm (94%)	0.30 μm (93%)	0.25 μm (65%)	0.5 μm (90%)
1250°C/3 h	25 μm (85%)	2.0 μm (95%)	15 μm (87%)	0.3 μm (68%)	1.0 μm (97%)

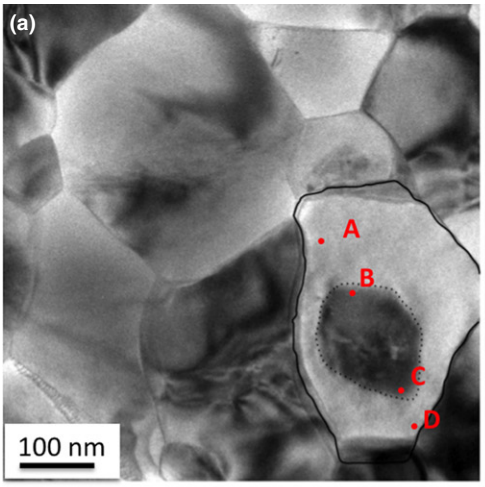

Position	A	B	C	D
Y (at.%)	0.72	0	0	0.78
Mg (at.%)	0.41	0.04	0.05	0.39

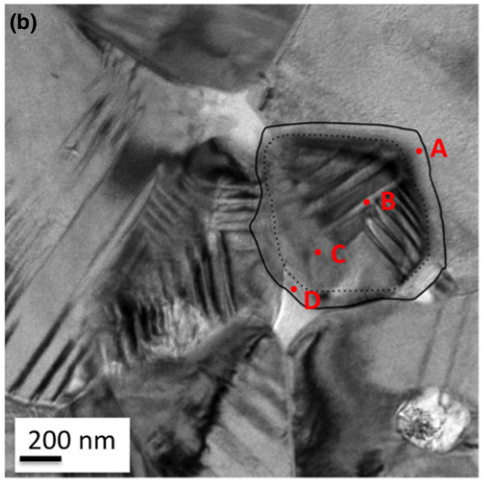

Position	A	B	C	D
Y (at. %)	1.32	0	0	1.74
Mg (at. %)	0.49	0	0	0.29

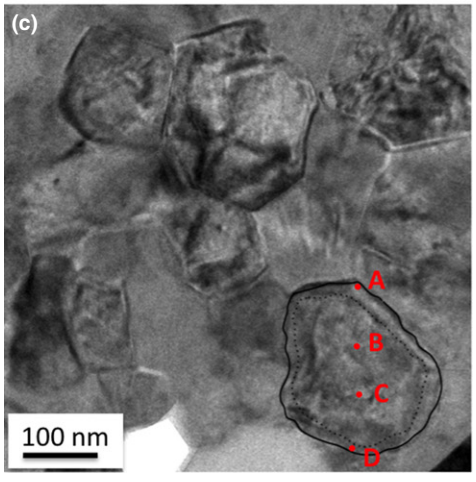

Position	A	B	C	D
Y (at.%)	0.38	0	0	0.29
Mg (at.%)	0.6	0	0	0.43

Fig. 9. TEM–EDS of $BaTiO_3$ codoped with MgO and Y_2O_3 sintered at 1150°C for 3 h, (a) 0.5Mg1Y, (b) 0.5Mg3Y, and (c) 1Mg1Y.

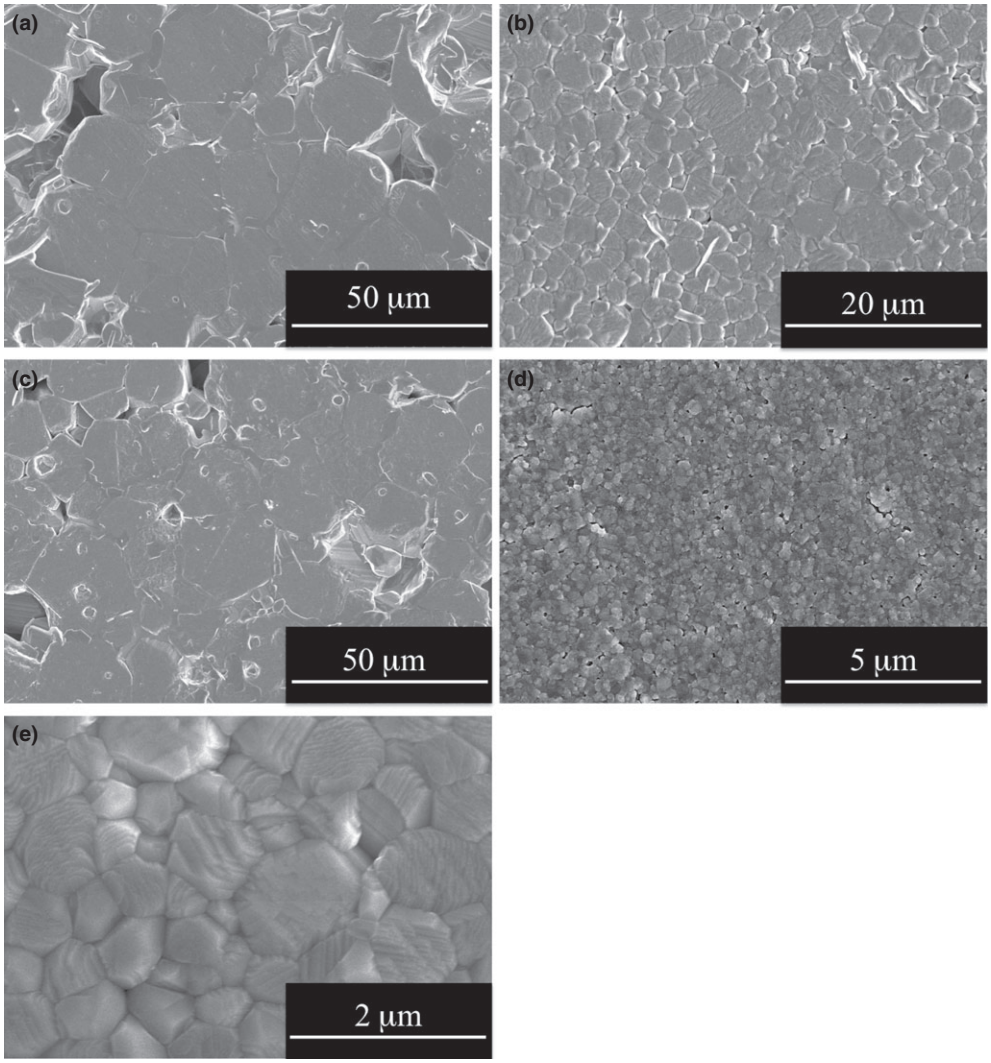

Fig. 10. SEM micrographs of $BaTiO_3$ codoped with MgO and Y_2O_3 sintered at 1250°C for 3 h, (a) 0.5Mg1Y, (b) 0.5Mg3Y, (c) 1Mg1Y, (d) 1Mg3Y, and (e) $BaTiO_3$.

References

[1]G. Arlt, D. Hennings, and G. D. With, "Dielectric Properties of Fine-Grained Barium Titanate Ceramics," *J. Appl. Phys.*, **58** [4] 1619–25 (1985).

[2]I. W. Chen and X. H. Wang, "Sintering Dense Nanocrystalline Ceramics Without Final-Stage Grain Growth," *Nature*, **404**, 168–71 (2000).

[3]X. H. Wang, X. Y. Deng, H. L. Bai, H. Zhou, W. G. Qu, and L. T. Li, "Two-Step Sintering of Ceramics with Constant Grain-Size, II: $BaTiO_3$ and Ni-Cu-Zn Ferrite," *J. Am. Ceram. Soc.*, **89** [2] 438–43 (2006).

[4]Y. H. Han, J. B. Appleby, and D. M. Smyth, "Calcium as an Acceptor Impurity in $BaTiO_3$," *J. Am. Ceram. Soc.*, **70** [2] 96–100 (1987).

[5]J. G. Park, T. S. Oh, and Y. H. Kim, "Dielectric Properties and Microstructural Behavior of B-Site Calcium-Doped Barium Titanate Ceramics," *J. Mater. Sci.*, **27**, 5713–9 (1992).

[6]J. Zhi, A. Chen, Y. Zhi, P. M. Vilarinho, and J. L. Baptista, "Incorporation of Yttrium in Barium Titanate Ceramics," *J. Am. Ceram. Soc.*, **82** [5] 1345–8 (1999).

[7]T. Nagai, K. Iijima, H. J. Hwang, M. Sando, T. Sekino, and K. Niihara, "Effect of MgO Doping on the Phase Transformations of $BaTiO_3$," *J. Am. Ceram. Soc.*, **83** [1] 107–12 (2000).

[8]R. E. Eitel, C. A. Randall, T. R. Shrout, P. W. Rehrig, W. Hackenberger, and S. E. Park, "New High Temperature Morphotropic Phase Boundary Piezoelectrics Based on $Bi(Me)O_3$–$PbTiO_3$ Ceramics," *Jap. J. Appl. Phys.*, **40**, 5999–6002 (2001).

[9]H. Kishi, Y. Okino, M. Honda, Y. Iguchi, and M. Imaeda, "The Effect of MgO and Rare-Earth Oxide on Formation Behavior of Core-Shell Structure in $BaTiO_3$," *Jpn. J. Appl. Phys.*, **36**, 5954–7 (1997).

[10]D. Makovec, Z. Samardzija, and M. Drofenik, "Solid Solubility of Holmium, Yttrium, and Dysprosium in $BaTiO_3$," *J. Am. Ceram. Soc.*, **87** [7] 1324–9 (2004).

[11]Y. H. Song, J. H. Hwang, and Y. H. Han, "Effects of Y_2O_3 on Temperature Stability of Acceptor-Doped $BaTiO_3$," *Jap. J. Appl. Phys.*, **44** [3] 1310–3 (2005).

[12]C. H. Kim, K. J. Park, Y. J. Yoon, D. S. Sinn, Y. T. Kim, and K. H. Hur, "Effects of Milling Condition on the Formation of Core-Shell Structure in $BaTiO_3$ Grains," *J. Euro. Ceram. Soc.*, **28**, 2589–96 (2008).

[13]J. S. Park, M. H. Yang, and Y. H. Han, "Effects of MgO Coating on the Sintering Behavior and Dielectric Properties of $BaTiO_3$," *Mater. Chem. Phys.*, **104**, 255–61 (2007).

[14]S. C. Jeon, C. S. Lee, and S.-J. L. Kang, "The Mechanism of Core/Shell Structure Formation During Sintering of $BaTiO_3$-Based Ceramics," *J. Am. Ceram. Soc.*, **95**, 2435–8 (2012).

[15]C. J. Peng and H. Y. Lu, "Compensation Effect in Semiconducting Barium Titanate," *J. Am. Ceram. Soc.*, **71** [1] C-44–6 (1988).

[16]C. J. Ting, C. J. Peng, H. Y. Lu, and S. T. Wu, "Lanthanum-Magnesium and Lanthanum-Manganese Donor-Acceptor-Codoped Semiconducting Barium Titanate," *J. Am. Ceram. Soc.*, **73** [2] 329–34 (1990).

[17]M. H. Lin and H. Y. Lu, "Site-Occupancy of Yttrium as a Dopant in BaO-Excess $BaTiO_3$," *Mater. Sci. and Eng.*, **335**, 101–8 (2002). □